AD-A256 020

‖‖ ‖‖‖‖ ‖‖ ‖‖‖‖ ‖‖

A Multiple-Aperture Multiple-Beam EHF Antenna for Satellite Communications

DTIC
ELECTE
OCT. 0. 7. 1992
S B D

L.W. Rispin
D.S. Besse

13 August 1992

Lincoln Laboratory

MASSACHUSETTS INSTITUTE OF TECHNOLOGY

LEXINGTON, MASSACHUSETTS

92 10 6 014

92-26526

‖‖‖‖‖‖‖‖‖‖‖‖‖‖‖‖‖

This report is based on studies performed at Lincoln Laboratory, a center for research operated by Massachusetts Institute of Technology. The work was sponsored by the Department of the Air Force under Contract F19628-90-C-0002.

This report may be reproduced to satisfy needs of U.S. Government agencies.

The ESD Public Affairs Office has reviewed this report, and it is releasable to the National Technical Information Service, where it will be available to the general public, including foreign nationals.

This technical report has been reviewed and is approved for publication.

FOR THE COMMANDER

Hugh L. Southall

Hugh L. Southall, Lt. Col., USAF
Chief, ESD Lincoln Laboratory Project Office

MASSACHUSETTS INSTITUTE OF TECHNOLOGY
LINCOLN LABORATORY

A MULTIPLE-APERTURE MULTIPLE-BEAM
EHF ANTENNA FOR SATELLITE COMMUNICATIONS

L.W. RISPIN
D.S. BESSE
Group 64

TECHNICAL REPORT 957

13 AUGUST 1992

LEXINGTON   MASSACHUSETTS

ABSTRACT

Measurements on an experimental model of a 127-beam multiple-aperture EHF antenna are reported. Featuring a hexagonal arrangement of seven individual multiple-beam lens antennas, the 44-GHz antenna array was designed for adaptive nulling applications in which 14 beams could be accessed to simultaneously provide 1.5° theater coverage and two independent agile beams. Antenna pattern and gain measurements for all 127 beams and results from simulated nulling experiments using a simple mechanically driven weighting network are discussed. Null depths of 30 dB and nulling resolutions of 0.1° are shown. The measurement results support the viability of this type of adaptive antenna system.

iii

ACKNOWLEDGMENTS

TABLE OF CONTENTS

LIST OF ILLUSTRATIONS

1. INTRODUCTION

A promising configuration for an adaptive antenna involves interspersing the antenna patterns of several individual multiple-beam antennas (MBAs) to provide complete global coverage. Overlapping beam coverage is obtained without the usual penalty on the gain of individual beams normally associated with a single aperture MBA. Due to their origination from spatially separated MBAs, adjacent beams have large phase slopes with respect to one another, which can yield high degrees of nulling resolution.

Results from measurements conducted on an experimental model of an antenna designed to exploit these advantages are discussed here. Featuring a hexagonal arrangement of seven individual 8-inch-lens MBAs, the antenna system provides 127 highly overlapped beams to cover the earth from synchronous orbit. Intended for use with a nulling network that has 14 input channels and three output channels, the envisioned antenna system would be capable of providing a single 1.5° theater coverage and two independent agile beams. Null depths exceeding 30 dB and very narrow null widths offering resolution better than 0.1° were sought.

Antenna gain and pattern measurements were made on all 127 beams. With the aid of a four-channel nulling network utilizing mechanically driven attenuators and phase shifters, simulations were performed to examine the capabilities of a portion of the MBA in simulated adaptive nulling scenarios. Discussions of these measurements follow a brief description of the antenna.

1

2. DESIGN FOR 127-BEAM ADAPTIVE ANTENNA

2.1 Design Criteria and Beam Coverage

Earth coverage capability was desired from an array of beam patterns that would provide that each point on the earth could be served by any of at least three beams having minimum gain > 31 dBi. Adjacent beams would be associated with separate component antenna apertures to avoid the gain penalty associated with closely spaced beams that share a common aperture. Figure 1 shows a hexagonal array pattern of 127 beams and illustrates the minimum gain situation for three adjacent beams. Specifying > 31-dBi gain within a radius R implies the maximum beam radius of $R_{max} \leq 1.7°$. Consequently, to ensure a minimum gain ≥ 31 dBi for all three beams to a user located anywhere within a theater diameter of $d = 1.5°$, the beam spacing was chosen as,

$$\theta_s = 1.6° \quad \leq \quad \sqrt{3}\,(R_{max} - d/2) = (\theta_s)_{max}\,. \tag{1}$$

Spacing the beams at 1.6° intervals is consistent with the requirements of the minimum gain criteria and provides coverage over an 18° sector, corresponding to earth coverage from synchronous orbit.

Null depths formed by adaptive weighting of beams were desired to be at least 30 dB below the maximum gain of an individual beam. Specifying that adjacent beams emanate from separate antennas would produce relative phase slopes between beams, the effect of which would be to "sharpen" the nulls. It was desired that the adapted antenna gain recover to within −15 dB of the peak beam gain within 0.1° from a null. This "nulling resolution" corresponds to the minimum separation between a jammer and a user having an assumed link margin of 15 dB with respect to peak beam gain or approximately 9-dB margin at the edge of the beam pattern, where $G \approx 31$ dBi.

2.2 Adaptive Antenna System

A hexagonal arrangement of seven 8-inch-lens MBAs was used to implement the desired characteristics. Figure 2 illustrates the antenna and associated system. The central MBA assembly contributes 19 beams, while the six outer MBA assemblies contribute 18 beams each. Beams are accessed through either an 8:1 or an 11:1 switch tree in the former assembly and either an 8:1 or a 10:1 switch tree in the latter. Via these switching networks, two beams from each component MBA, 14 in all, are available to form appropriate beam patterns to cover either a theater and/or individual user terminals. Numerical designations for the 127 beams and the lens and switching networks associated with each beam are given in the array pattern in Figure 1.

An adaptive processor was envisioned that would combine the 14 signals to produce three output signals, one for the 1.5° theater area, and the other two for each of the independent "agile" beams. A slightly modified form of the Applebaum-Howells type of adaptive processor was considered. This featured the introduction of "user" filters in the feedback loop to reduce the influence of user signals on the adaption process.

3

200733-1

(a) MINIMUM GAIN CRITERIA

$G(R) \geq 31$ dBi

R = BEAM RADIUS

d = THEATER DIAMETER

θ_S = BEAM SPACING

R

d

θ_S

BEAM # — — LENS #

SWITCH TREE # —

TREE PORT #

95-4
7-4

(b) MULTIPLE-LENS ARRAY PATTERN

VIEW FROM SATELLITE
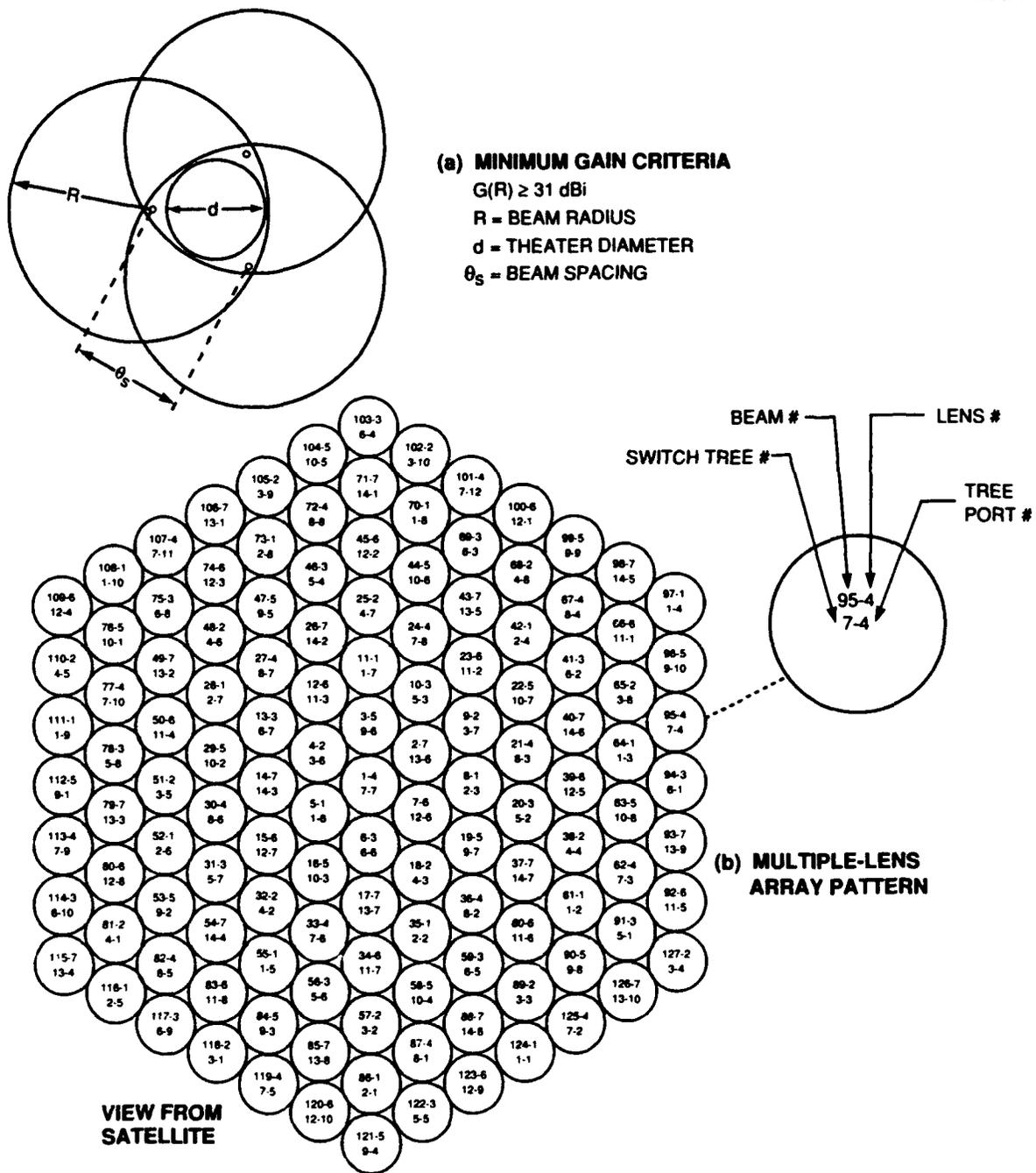
Figure 1. Array pattern for 127-beam antenna and illustration of minimum gain criteria.

4

(a) MECHANICAL LAYOUT

NETWORK BAY
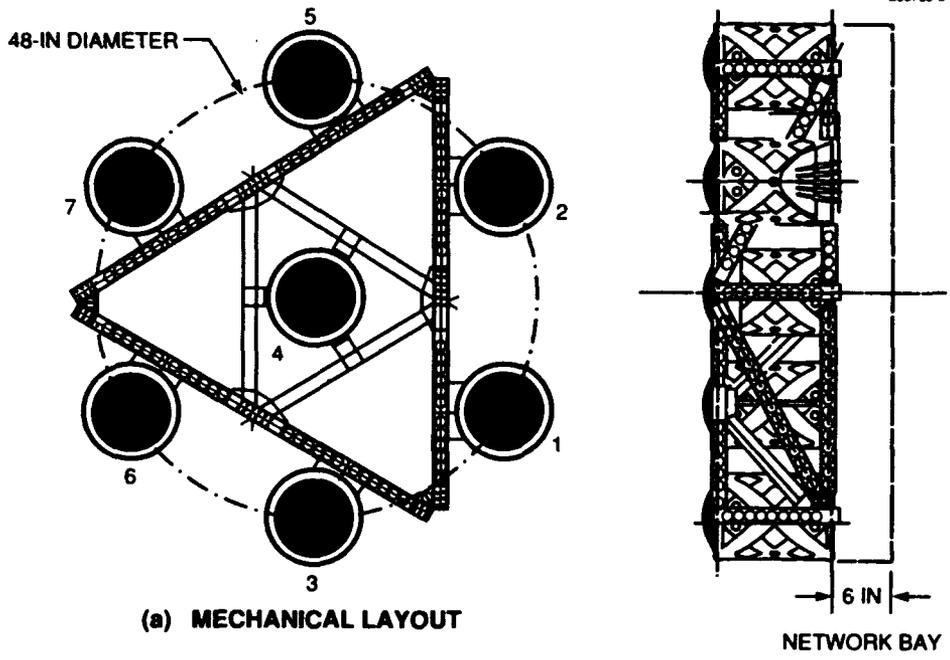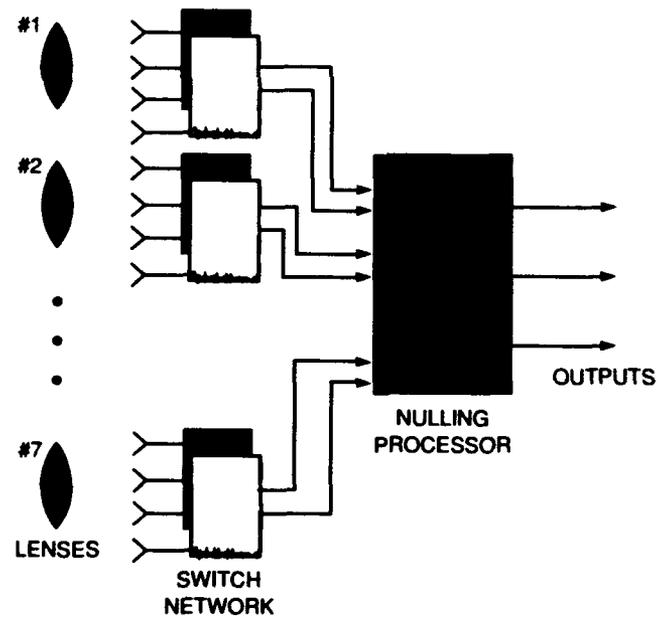
(b) ENVISIONED ADAPTIVE ANTENNA SYSTEM

Figure 2.   Multiple-lens 127-beam antenna array: (a) mechanical layout and (b) envisioned system architecture.

5

3. ANTENNA DESCRIPTION

3.1 Antenna Array

Figure 3 is a photograph of the experimental model of the multiple-lens MBA that was constructed. A lightweight aluminum framework supports the hexagonal arrangement of seven individual 8-inch-lens antennas. The weight of the entire antenna assembly is just under 56 lbs. The centers of the six outer lenses are evenly distributed on a 24-inch radius from the center of the array.

3.2 Individual Lens Antenna MBAs

Each lens antenna assembly is an MBA designed to provide either 18 or 19 beams having nominal beamwidths of 2.5° and nominal gains of 37.5 dBi. Design spacing between beams was 4.24°. Each assembly consists of an 8-inch-diameter dielectric lens fed by a cluster of 18 (or 19) dielectric rod loaded conical horns. Photographs of the central 19-beam MBA assembly and its feed are shown in Figure 4. The lens has a focal length of 12 inches, resulting in a F/D of 1.5. Machined from Rexolite^{TM} ($\epsilon_r = 2.54$), the flat and convex surfaces are "waffled" to simulate matching $\lambda/4$ transformers. In addition, the flat surface is "zoned" into two surfaces to reduce weight. The 2.94-inch-long conical horns open in a 15° flare angle to 0.83 inch in diameter and feature hollow dielectric rod inserts (outside diameter of 0.25 inch and wall thickness of 0.01 inch), which extend 2 inches beyond the horn opening. The rods increase the gain and narrow the beamwidth of the feed, subsequently producing the proper illumination at the lens to achieve the desired MBA gain and beamwidth. Right-hand circular (dielectric vane) polarizers are built into the tubular section of the feed.

3.3 Switch Tree Networks

Ferrite-switch tree networks attached to the waveguide ports of the conical feed horns allow for the selection of two beams from a particular lens. The central 19-beam assembly employs an 8:4:2:1 tree and an 11:7:4:2:1 tree. The 18-beam assemblies employ an 8:4:2:1 tree and a 10:6:3:2:1 tree. Separate drawings of the 8:1 and 10:1 switch trees are shown in Figure 5 along with a combined illustration showing how they appear together behind a feed horn cluster. Insertion loss thru any path of any switch tree was quoted to be a nominal 1.12 dB. Built by ElectroMagnetic Sciences, Inc. (EMS) these networks feature the use of lightweight 44-GHz switchable ferrite circulators interconnected by soldered flangeless electroformed WR-19 waveguide. Both switch tree networks for a particular lens fit within a 5.3-inch-long, 7.75-inch-diameter cylinder and weigh about 1 lb. Associations between beams, switch trees, and component MBA lens antenna assemblies were given in Figure 1.
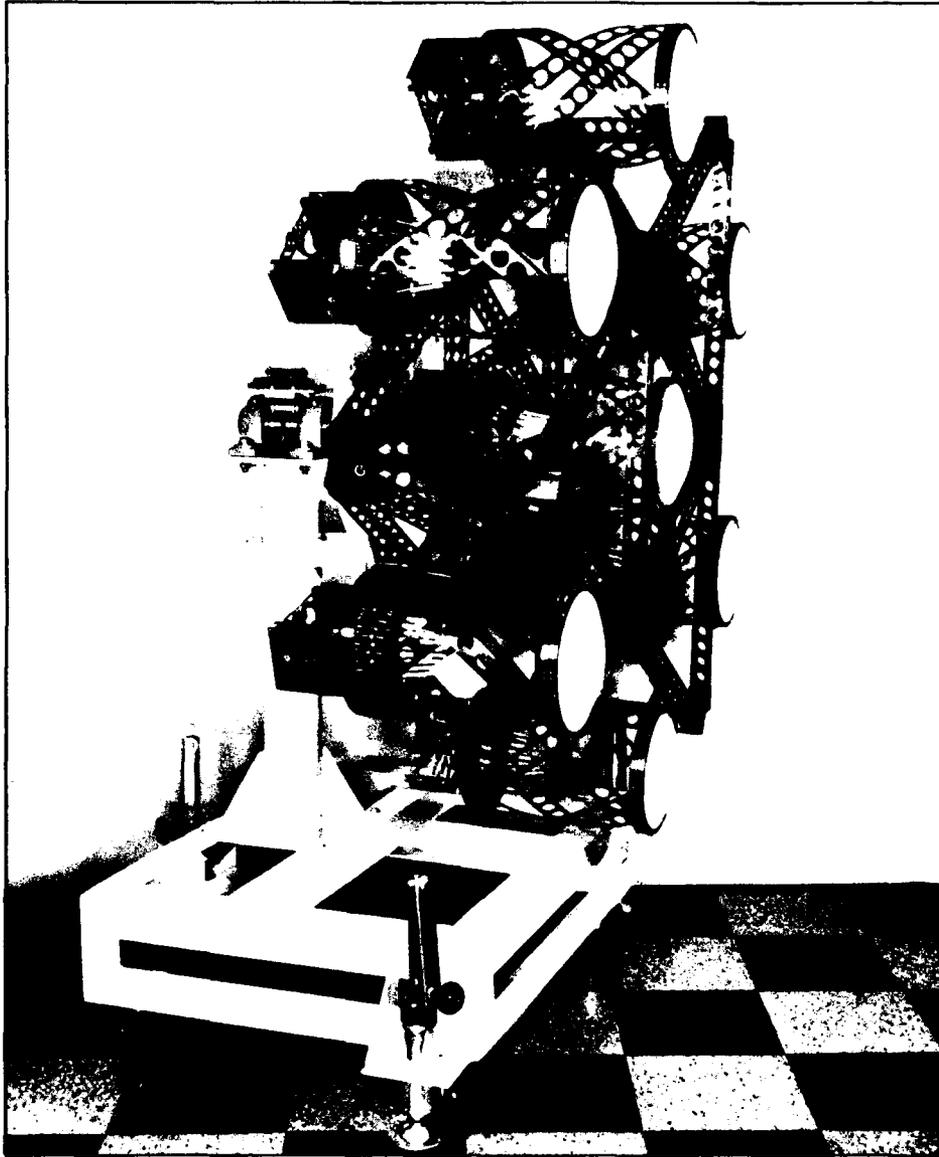
Figure 3. Photograph of the experimental model of the 127-beam antenna.

(a) SWITCH TREE ASSEMBLY

(b) FEED HORN CLUSTER

(c) ASSEMBLED MBA – 6.1 lb
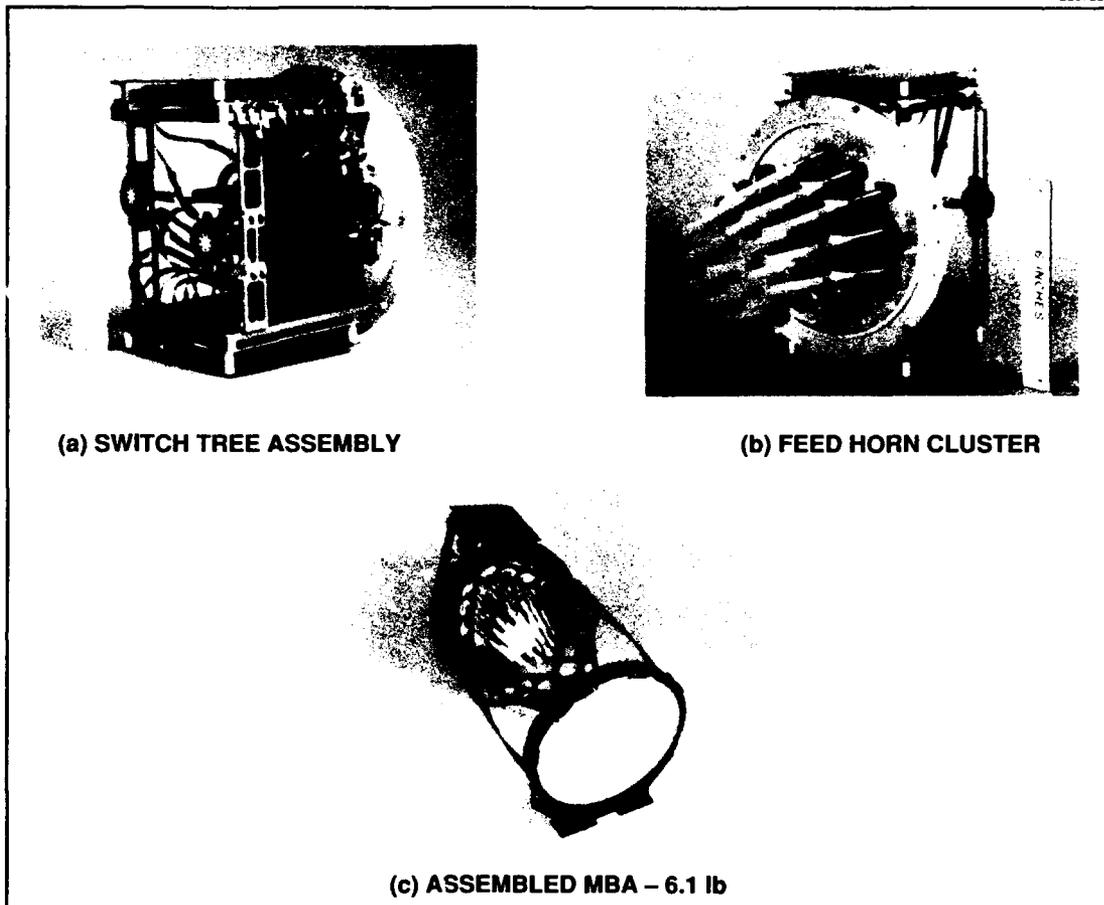
Figure 4. Several views of the central 19-beam MBA assembly.

(a) INTEGRATED 10:1 ASSEMBLY

(b) INTEGRATED 8:1 ASSEMBLY
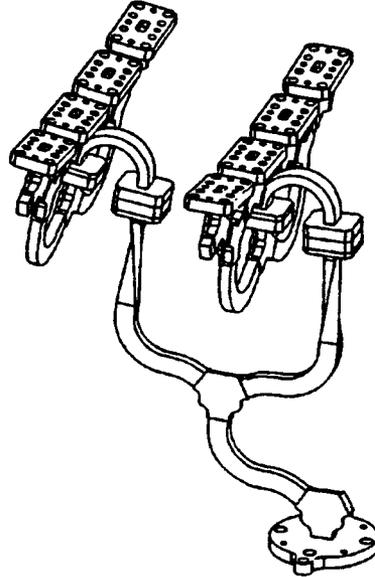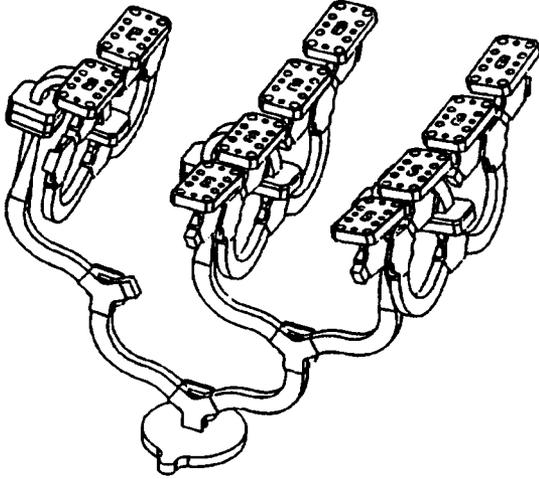
(c) 18:2 FINAL MICROWAVE ASSEMBLY
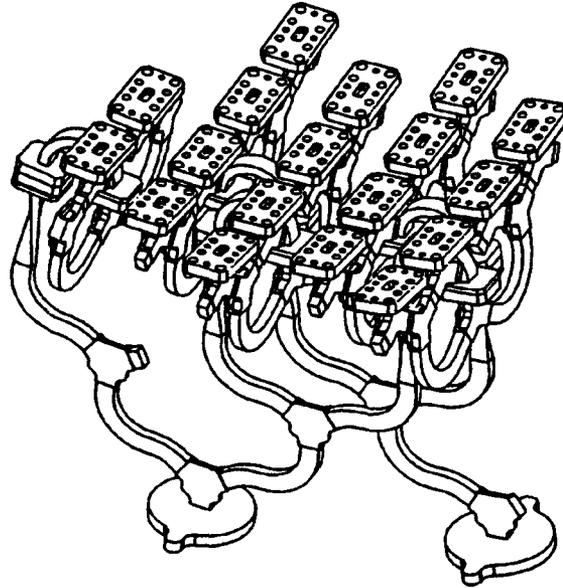
Figure 5.   Assemblies for the 18:2 switch tree network.

10

4. MEASUREMENT SYSTEM

4.1 Antenna Range

Measurements were performed in a compact range facility at the Lincoln Laboratory Antenna Test Range. Microwave absorbing material, pyramidal cones and flat panels, cover the walls, ceiling, and floor of the 40-x 20- x 17-ft-high room. The upper half of a 12-ft parabolic reflector (not including the serrated edge) is situated at one end of the room. Fed at its focal point by a circularly polarized scalar feed horn, this reflector provides a near planar wave over an approximately 6-ft-diameter area at the antenna. Axial ratio of the incident "plane wave" in this installation has been noted as being typically on the order of 0.5 dB or better.

The antenna was mounted on an elevation-over-azimuth positioner. Antenna pattern data was taken using the so-called "on-the-fly" technique, in which the antenna was first positioned in elevation and then swept in a continuous motion in azimuth. Based upon information from synchro-encoders, at the intended azimuth positions, the receiver was triggered and data recorded. Accuracy associated with this technique is quoted to be approximately ±10 percent of the azimuth increment. There were also indications of small elevation errors that were somewhat cumulative in nature. The primary effect of these errors will be seen in Section 6, as small shifts in the pattern with respect to elevation. Fortunately, however, the errors are uniformly small enough to avoid introducing any significant distortion into the antenna patterns.

4.2 Four-Channel Nulling Network

To assess the nulling performance of the antenna array, a four-channel nulling network was constructed from readily available components. Each channel employed a mechanically driven attenuator and phase shifter to simulate weighting factors varying from 0 to −40 dB in amplitude and from 0° to 360° in phase. Both the attenuator and the phase shifter were set by stepper motors, which could be controlled remotely from the measurement console. Waveguide shims were inserted at appropriate places to match the individual channel path lengths as closely as possible. A limited number of available attenuators and phase shifters, as well as their considerable size, led to the decision to implement only four channels. Components of the nulling network were mounted on an aluminum plate, which can be seen within the antenna support structure in Figure 6.

4.3 Four-Beam Adaptive Array

Beams 1, 2, 3, and 4 were used, in conjunction with the four-channel nulling network, to demonstrate the capabilities of the antenna. These beams are located adjacent to one another near the center of the array pattern (see Figure 1). Their relative positions were thought to be representative of a typical four-beam situation. Comparable lengths ($\approx$ 30 inches) of waveguide were fabricated and inserted between the respective output flanges to the input ports of the nulling network. Waveguide shims were included to more precisely match the individual path lengths.

11
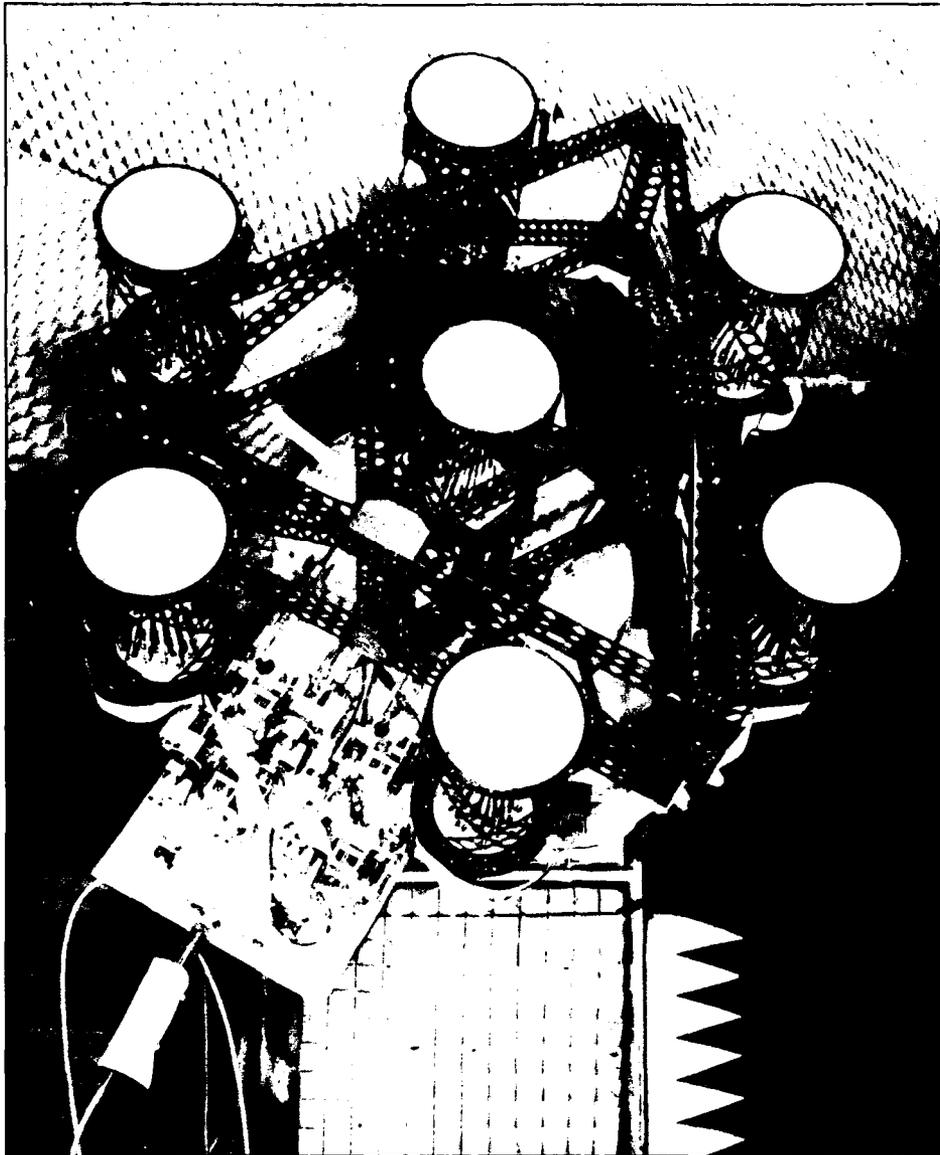
Figure 6. Photograph of multiple-lens MBA and four-channel mechanically driven nulling network in the compact range facility.

4.4 Test Procedure and Nulling Algorithm

The nulling process was simulated by using measured channel (beam) levels in a simple matrix inversion algorithm to determine suitable adaptive weights. Successively positioning the antenna to the coordinates of each assumed jammer, signal levels were measured on each of the four channels at five evenly spaced frequencies between 43.5 and 45.5 GHz. A four-element sample matrix $\underline{\Phi}_j(f_i)$ was formed from the channel levels for each frequency, f_i, and each assumed jammer, j. Covariance matrices for the interfering jammers were determined from,

$$\underline{\underline{R}}_j(f_i) = \underline{\Phi}_j^*(f_i)\underline{\Phi}_j^T(f_i) \tag{2}$$

where the superscripts indicate complex conjugation and transposition. An average covariance matrix was defined by,

$$\underline{\underline{R}} = \sum_{j=1}^{\#jammers} \sum_{i=1}^{5} \underline{\underline{R}}_j(f_i). \tag{3}$$

A small noise level was added to the main diagonal of the average covariance matrix to avoid the possibility of a singular matrix. Subsequently, "adaptive" weights were calculated from,

$$\underline{w} = \underline{\underline{R}}^{-1}\underline{Q} \tag{4}$$

where $\underline{Q}$ specifies the desired quiescent pattern weights or steering vector. The calculated weights were appropriately normalized in magnitude and phase.

Upon setting the attenuators and phase shifters in the four-channel nulling network in accordance with these weights, the opportunity was usually taken to measure null depth, while the antenna was still oriented in the direction of the last assumed jammer. Antenna pattern measurements commenced thereafter. Raster scan measurements of the adapted patterns in the vicinity of the jammers were usually made over 0.6° × 0.6° windows using 0.02° measurement increments in order to examine the detail characteristics of the nulls formed. Measurements were also made over 5° × 5° windows at 0.1° measurement increments in the area of the desired quiescent pattern.

13

5. MEASUREMENTS: INDIVIDUAL BEAMS

5.1 Beam Patterns

Prior to assembling the component MBAs onto their common frame, pattern measurements were made for each of the beams associated with each MBA. Data was taken at 44.5 GHz over a 5° × 5° window in 0.25° increments. Figure 7 shows the pattern contours of the beams associated with the central MBA assembly. A nominal beamwidth of 2.5° was observed for all 127 beams.

5.2 Beam Peak Locations and Gain

During assembly of the component MBAs onto their lightweight frame, shims were used at the points of attachment to effect the desired alignment between their respective beam patterns. Once secured, the coordinate positions corresponding to the peak gain for each beam was determined via careful manual positioning of the antenna. The observed beam positions are illustrated in Figure 8 by 1.6° diameter circles centered about the measured peak locations. Overall alignment is good. Small alignment errors would not be expected to have a significant effect on adaptive nulling performance. On the other hand, the validity of the minimum gain criteria in Section 2.1 does require reasonable accuracy with regard to the alignment of the beams.

Gain measurements were facilitated by temporarily mounting a "calibrated" scalar horn on the side of the MBA space frame, directed at right angles to the main axis of the array. The test mixer was connected to the output of the scalar horn for calibration (at 43.5 to 45.5 GHz in 0.1 GHz steps) and then to the output port of a switch tree for measurement. The MBA was successively positioned to the previously determined coordinates corresponding to a beam peak, the switch tree configured to address that beam, and the receiver response was recorded. Figure 9 shows the mean (bounded above and below by the standard deviation) of the measured gain for the beams associated with each of the seven lens assemblies. Average measured gains at the switch network outputs are between 36 and 36.5 dBi across the frequency band. Although not exhaustive, these measurements tend to indicate that the individual MBA assemblies appear to exhibit predicted performance.

5.3 Minimum Gain Criteria

From pattern measurements, beam patterns are down almost 6 dB from peak at a radius $R = 1.7°$. Gain measured at the switch network outputs was typically between 36 and 36.5 dBi. Hence, allowing for a loss of 1.1 dB in the switch network, it appears that minimum gain criteria,

$$\text{Beam Gain} \geq 31 \text{ dBi at } R = 1.7° \tag{5}$$

has been achieved, at least in a general sense. A more definite confirmation would require more intensive measurements.

15
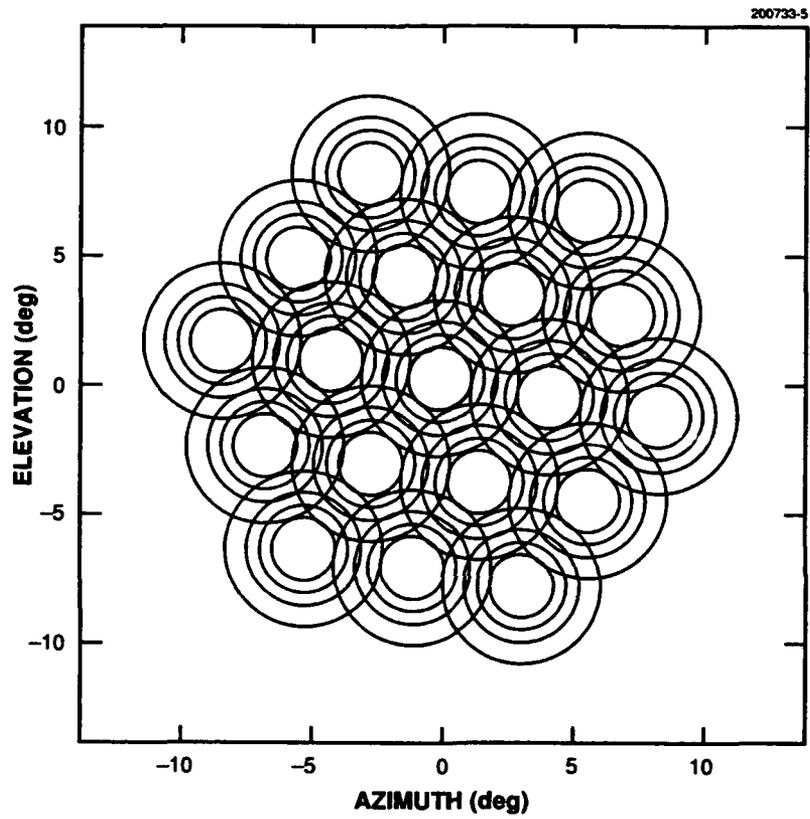
Figure 7. *Antenna pattern contours (-3, -6, -10, and -20 dB) for beams associated with the central 19-beam lens MBA.*

16
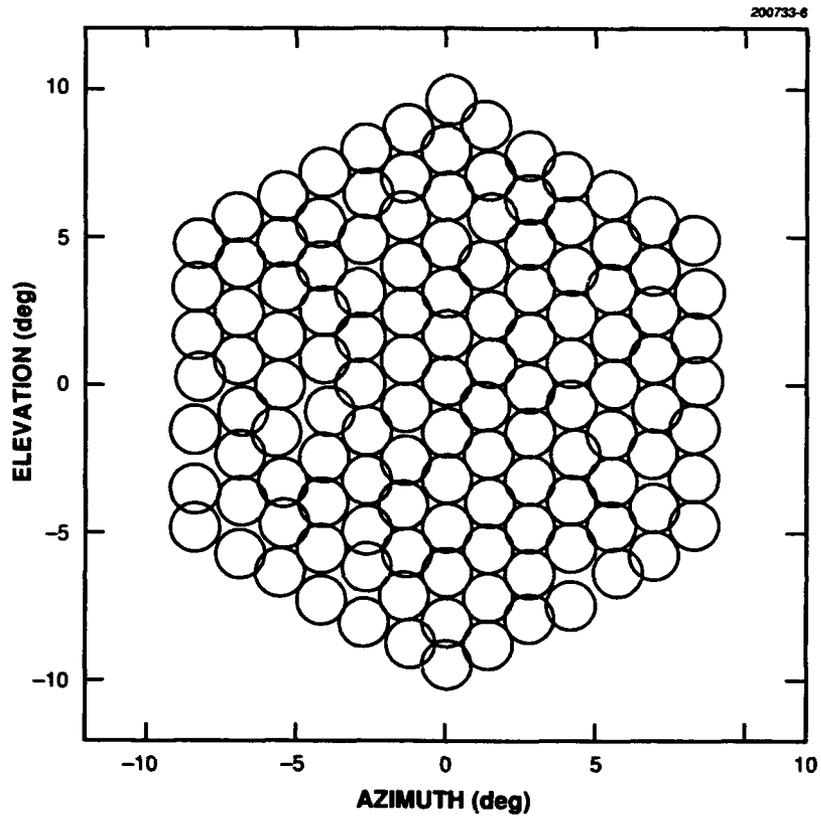
*Figure 8.* Array pattern simulated by 1.6° diameter circles at measured beam peak locations.
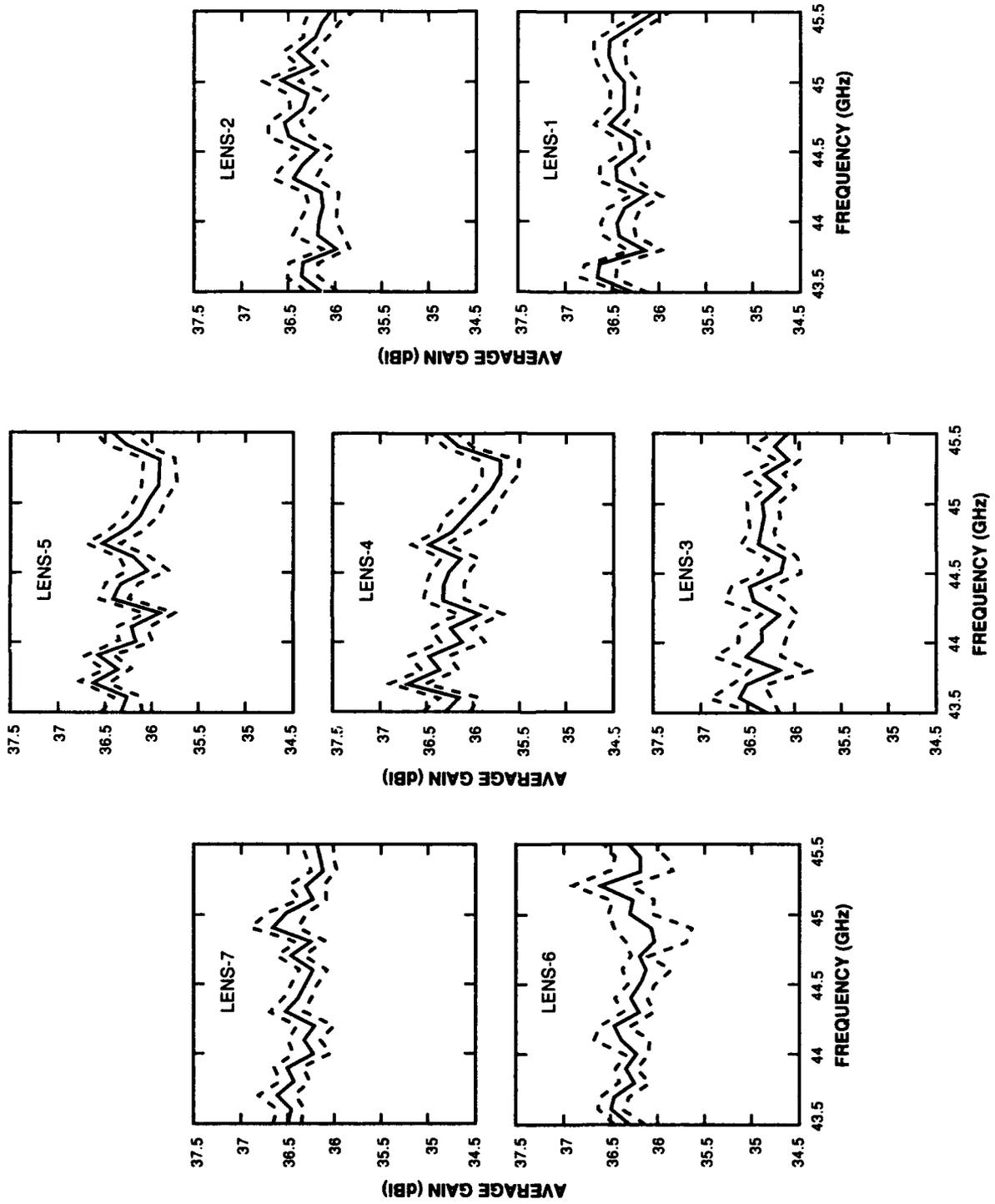
Figure 9. Average gain measured at the switch network outputs for the beams associated with each lens assembly. Gain at one standard deviation is shown dashed.

18

6. MEASUREMENTS: SIMULATED NULLING SCENARIOS

6.1 Single Jammer Assumed

A full-band jammer was assummed to be located at (Az = −0.4°, El = +0.85°), which is roughly equidistant from the peaks of beams 1, 2, and 3. Following the simulation procedure described in Section 4.4, signal channel levels were measured and weights calculated with beam 2 defined as the quiescent pattern. This scenario is illustrated in Figure 10. All measured results are normalized to the peak gain of the quiescent pattern, beam 2. Contours of the desired quiescent pattern and jammer location are indicated in Figure 10(a). The adapted pattern is shown in Figure 10(b). Only those contours 15 dB or more below the peak quiescent level are shown in order to emphasize the coverage area. The 6 dB pattern contour of the quiescent beam (corresponding to a gain of ≈ 31 dBi) is shown dashed to illustrate the quiescent pattern coverage area. A contour plot of the adapted pattern in the vicinity of the jammer is shown in Figure 10(d). A nulling resolution of 0.1° is observed in most directions away from the jammer. The apparent shift of the null from the desired location results from positioner-controller errors associated with the "on-the-fly" measurement technique discussed in Section 4. In Figure 10(c), an azimuth cut through the adapted pattern (for 44.5 GHz) at the jammer elevation shows null depth approaching 30 dB. Figure 10(e) indicates null depth to be a nominal 30 dB across the band.

6.2 Two Full-Band Jammers Assumed

Full-band jammers were assumed located at (Az = −0.4°, El = +0.85°) and (Az = +0.4°, El = +0.85°), the former position roughly equidistant from the peaks of beams 1, 2, and 3, and the latter roughly equidistant from the peaks of beams 1, 3, and 4. Weights were calculated with beam 1 defined as the desired quiescent pattern. Measurement results are shown in Figure 11. Again, the data is normalized to the peak gain of the quiescent pattern, beam 1. Jammer locations and contours of the desired quiescent pattern are shown in Figure 11(a). Contours of the adapted antenna pattern that are 15 dB or more below the peak quiescent level are shown in Figure 11(b). The remaining area above this assumed link margin level is clearly evident. The 6-dB pattern contour (G ≈ 31 dB) for the quiescent beam is shown dashed to illustrate the quiescent pattern coverage area. Contour plots of the adapted pattern in the vicinities of both jammers in Figures 11(d) and 11(e), show nulling resolutions better than the desired 0.1° in most directions away from the respective jammers. Again, the small shifts in the null positions are related to positioner-controller problems. Nulls were formed at both desired locations where signal levels had been sampled. In Figure 11(e), both nulls are seen to exceed 30 dB (below the quiescent peak) in the azimuth cut at the jammer elevation through the adapted pattern at 44.5 GHz. Figures 11(f) and 11(g) show the null depths to generally exceed the 30-dB level across most of the band.

19
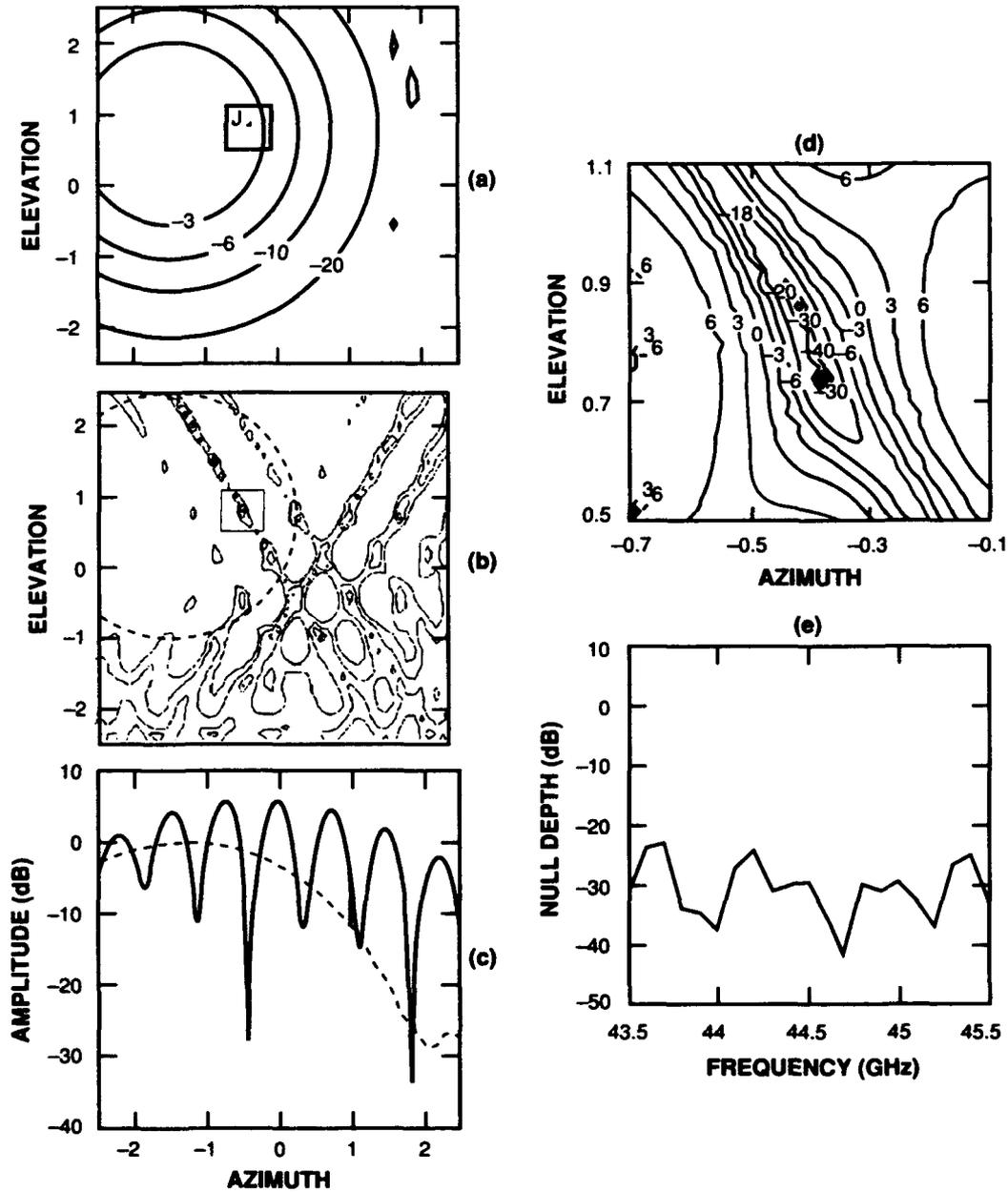
Figure 10. Single jammer scenario, data is normalized to quiescent peak: (a) quiescent pattern, (b) adapted pattern in coverage area, (c) azimuth cut through null, (d) close-up of vicinity about jammer, and (e) null depth.
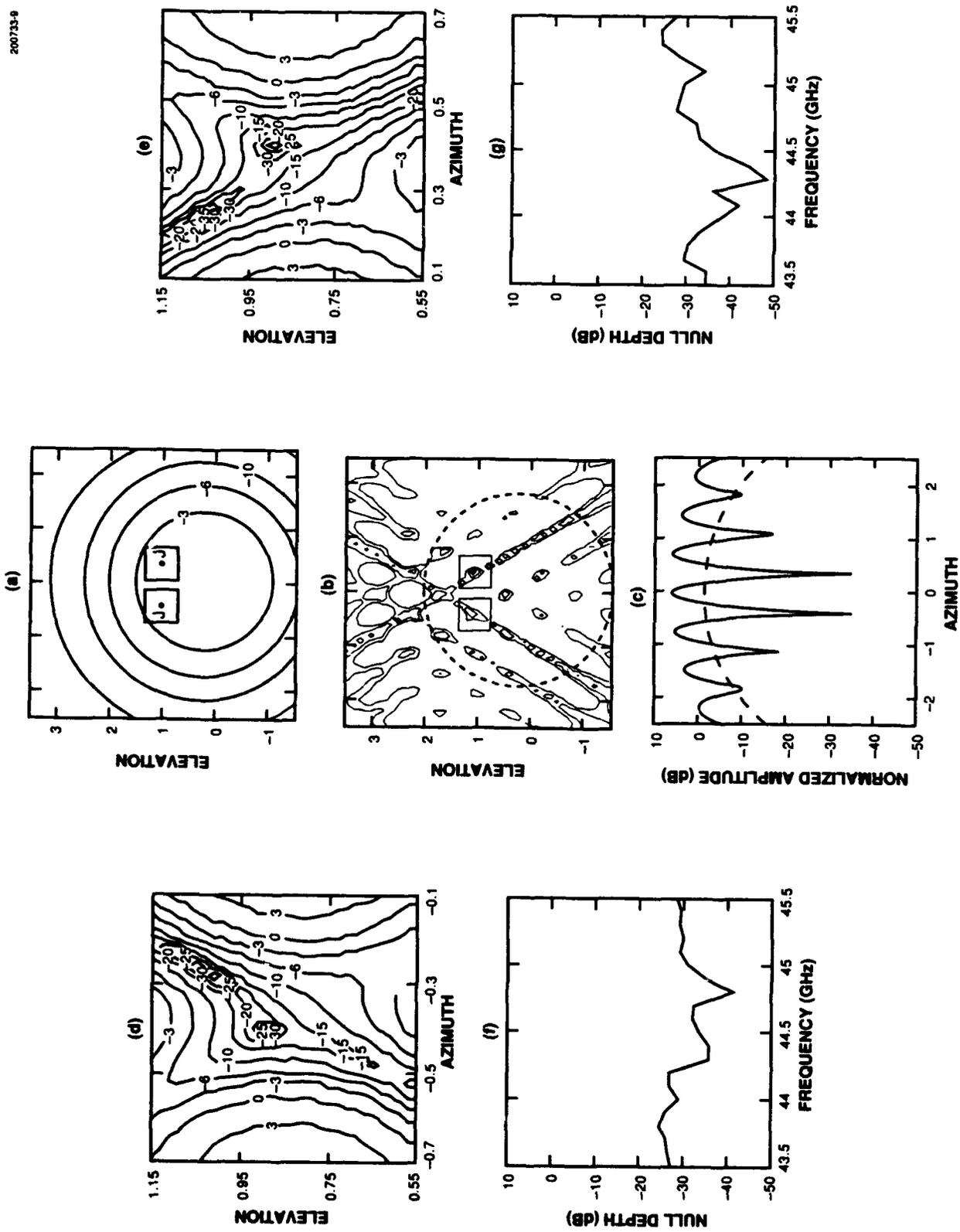
Figure 11. Two jammer scenario, data is normalized to quiescent peak: (a) quiescent pattern, (b) adapted pattern in coverage area, (c) azimuth cut through nulls, (d) and (e) close-up of vicinities about jammers, and (f) and (g) null depths.

21

7. CONCLUSIONS

Preliminary antenna testing of a 127-beam multiple-lens adaptive array has indicated levels of performance commensurate with design criteria. Although time did not permit exhaustively detailed measurements, due to the large number of beams involved, the data indicate that design goals have been achieved.

Pattern and gain measurements revealed nominal beamwidths of about 2.5° and nominal gains of 37 to 37.5 dBi for all 127 beams. Measurements also indicated the capability for the antenna to satisfy the minimum gain requirement of 3i dB for any point in the earth field-of-view by any one of three beams. Implicit in the minimum gain criteria, however, is the sufficiently precise alignment of the beams.

Some basic characteristics of adaptive antenna performance were examined in simulated nulling experiments involving four of the beams. The antenna demonstrated its ability to produce sharp nulls generally exceeding –30 dB across the frequency band. Nulling resolution defined by the the minimum angular separation between a user and a jammer was generally better than the desired 0.1°. Realistically, the four-beam nulling simulations are perhaps more representative of point-to-point situations than they are of theater coverage, which would probably involve a greater number of beams. In this regard, it can also be assumed that the performance exhibited in the four-beam nulling simulations tends to underestimate the capabilities of a more complete complement of beams (seven, for example) that would probably be used to provide theater coverage. Further, a more sophisticated electronic nulling network could be expected to yield a somewhat better performance. Hence, the nulling performance described here using the mechanical network, in all likelihood, understates the potential capabilities of the 127-beam multiple-lens array.

REPORT DOCUMENTATION PAGE

1. AGENCY USE ONLY (Leave blank)	2. REPORT DATE 13 August 1992	3. REPORT TYPE AND DATES COVERED Technical Report

4. TITLE AND SUBTITLE

A Multiple-Aperture Multiple-Beam EHF Antenna for Satellite Communications

6. AUTHOR(S)

Lawrence W. Rispin and David S. Besse

5. FUNDING NUMBERS

C — F19628-90-0002
PE — 33110F, 33603F, 33110F, 63226E
PR — 370

7. PERFORMING ORGANIZATION NAME(S) AND ADDRESS(ES)

Lincoln Laboratory, MIT
P.O. Box 73
Lexington, MA 02173-9108

8. PERFORMING ORGANIZATION REPORT NUMBER

TR-957

9. SPONSORING/MONITORING AGENCY NAME(S) AND ADDRESS(ES)

HQ AF Space Systems Division
SD/MHE
Los Angeles AFB, CA 90009-2960

10. SPONSORING/MONITORING AGENCY REPORT NUMBER

ESC-TR-92-072

11. SUPPLEMENTARY NOTES

None

12a. DISTRIBUTION/AVAILABILITY STATEMENT

Approved for public release; distribution is unlimited.

12b. DISTRIBUTION CODE

13. ABSTRACT (Maximum 200 words)

Measurements on an experimental model of a 127-beam multiple-aperture EHF antenna are reported. Featuring a hexagonal arrangement of seven individual multiple-beam lens antennas, the 44-GHz antenna array was designed for adaptive nulling applications in which 14 beams could be accessed to simultaneously provide 1.5° theater coverage and two independent agile beams. Antenna pattern and gain measurements for all 127 beams and results from simulated nulling experiments using a simple mechanically driven weighting network are discussed. Null depths of 30 dB and nulling resolutions of 0.1 are shown. The measurement results support the viability of this type of adaptive antenna system.

14. SUBJECT TERMS

antenna measurement	multiple aperture	EHF antenna
MBA	nulling antenna	satellite antenna
multiple beam		

15. NUMBER OF PAGES 36

16. PRICE CODE

17. SECURITY CLASSIFICATION OF REPORT Unclassified	18. SECURITY CLASSIFICATION OF THIS PAGE Unclassified	19. SECURITY CLASSIFICATION OF ABSTRACT Unclassified	20. LIMITATION OF ABSTRACT SAR